

# POTENTIAL OF HYPERSPECTRAL DATA FOR THE CLASSIFICATION OF VITD SOIL CLASSES

Sun-Hwa Kim, Jung-Rim Ma, Kyu-Sung Lee, Yang-Dam Eo\* and Yong-Woong Lee\*

Department of Geoinformatic Engineering, Inha University,  
253 Younghyun-dong, Incheon, 402-751, Korea  
Tel: +82-32-860-8805, e-mail: 22032128@inhaian.net

\*Agency for Defense Development P. O. Box 35, Yusong, Daejeon, KOREA

## ABSTRACT:

Hyperspectral image data have great potential to depict more detailed information on biophysical characteristics of surface materials, which are not usually available with multispectral data. This study aims to test the potential of hyperspectral data for classifying five soil classes defined by the vector product interim terrain data (VITD). In this study, we try to classify surface materials of bare soil over the study area in Korea using both hyperspectral and multispectral image data. Training and test samples for classification are selected with using VITD vector map. The spectral angle mapper (SAM) method is applied to the EO-1 Hyperion data and Landsat ETM+ data, that has been radiometrically corrected and geo-rectified. Higher classification accuracy is obtained with the hyperspectral data for classifying five soil classes of gravel, evaporites, inorganic silt and sand.

**KEY WORDS:** Hyperspectral, SAM, image classification, soil type, VITD, military map

## 1. INTRODUCTION

With many continuous narrow spectral bands, hyperspectral image data have shown great potential to extract more detailed and accurate information on various surface materials. Among many application fields of hyperspectral data, the main use of the high spectral resolution data would be the extraction of quantitative information related to the biophysical and chemical conditions of various surface materials. Perhaps, rock and vegetation are two primary targets that had been analysed by hyperspectral data. Although there have been a few hyperspectral-sensing studies related to the mapping of soil type, wetness, and organic contents (Ben-Dor et al., 2002; Meer, 2003), it is still rare to find such studies proving the true benefit of hyperspectral data for obtaining soil-related information over multispectral data. Spectral angle mapper (SAM) and spectral matching filtering method are used for soil type mapping (Crosta et al., 1998; Chabrilat et al., 2000; Nash et al. 2004).

As the first space-borne hyperspectral sensor, the EO-1 Hyperion imaging spectrometer has 242 spectral bands ranging from 400 to 2,500nm wavelength and 30 spatial resolution. Although data acquisition of Hyperion has been rather limited by the experimental operation of the satellite, the hyperspectral data have already been used for several studies related to geological and mineral mapping (Kruse et al., 2003; Nash et al. 2004).

The vector product interim terrain data (VITD) is a digitised map of conventional 1:50,000-scale military terrain analysis map produced by the US Army. The map is comprised of six thematic layers including obstacles, surface drainage, transportation, surface materials (soils),

surface configuration (slope) and vegetation. Since the mapping of these layers has been relied on aerial photographs and field survey, the map information is often outdated. The objective of this study is to test the potential of hyperspectral data for classifying five soil classes defined by the VITD.

## 2. STUDY SITES AND DATA USED

### 2.1 Study sites

To include more soil types, we select two study sites where the main cover types are bare soil and rock with minimum vegetation. Site 1 is Yang-Ju area in central part of the Korean peninsula. As seen in Figure 1, the study site 1 covers two major cover types of forest and rice paddy. This area includes four major soil classes defined by the VITD and their characteristics are listed in Table 1.

Table 1. The VITD soil classes included in the study area.

| Code | Soil types                                  |
|------|---|
| GM   | Silty gravels, gravel-sand-silt mixtures    |
| SM   | Silty sand, sand-silt mixture               |
| ML   | Inorganic silts and very fine sands         |
| CL   | Inorganic clays of low to medium plasticity |
| EV   | Evaporites                                  |

The study site 2 is selected for the detection of a particular soil type (evaporites) by the VITD soil types classes. The evaporites is a special soil type that is developed from dried tidal flats. Because of the spectral

similarity of evaporites and other bare soil types, the detection of the evaporites is often difficult. Hyperspectral data have already shown the capability of distinguishing soil salinity (Dehaan and Taylor, 2003). The study site 2 is located in southwest coastal region of the peninsular.

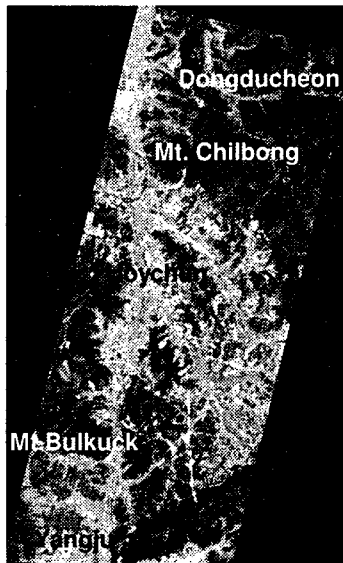


Figure 1. Location and major land cover types of site 1.

## 2.2 Data used

For the study, Hyperion imaging spectrometer data and Landsat ETM+ multispectral data were used (Table 2). To reduce any misclassifications due to the vegetation coverage, the both satellite data were chosen in early spring. Although the Hyperion data for the study site 2 was obtained during the leaf-off season, it didn't cause any problem since the evaporites soils are mostly non-vegetated.

Table 2. Hyperion and ETM+ data used for the two study sites.

| Data                     |            | Site 1        | Site 2       |
|--------------------------|------------|---------------|--------------|
| EO-1<br>Hyperion         | Date       | April 3, 2002 | June 3, 2001 |
|                          | Row*Col.   | 602*368       | 2438*895     |
|                          | # of bands | 242 bands     | 242 bands    |
|                          | Resolution | 30m           | 30m          |
| Land<br>-sat<br>ETM<br>+ | Date       | May 8, 2003   |              |
|                          | Row*Col.   | 605*372       | 2440*901     |
|                          | # of bands | 7 bands       |              |
|                          | Resolution | 28.5m         |              |

The VITD data of the study site 1 include four soil classes as shown in Figure 2. Soil type layer was extracted from the VITD map and used as reference data for selecting of training fields and test fields.

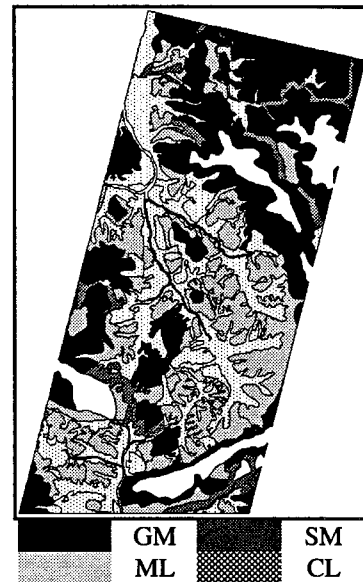


Figure 2. Soil type map (1:50,000 scale) of VITD at site 1.

## 3. METHODS

### 3.1 Pre-processing

For obtaining of more accurate spectral information, the hyperspectral data and multispectral data are atmospherically corrected using a radiative transfer model (MODTRAN). Although the atmospheric correction is not the essential step for the classification, it would be better for both hyperspectral and multispectral data to have almost the same level of radiometric quality. Once the Hyperion data were geo-rectified using a set of ground control points, the ETM+ data are then registered to the Hyperion data by image-to-image registration.

Hyperion data are further processed by the minimum noise fraction (MNF) transformation method. The MNF is modified version of principal component analysis method and used for minimizing of noise fractions, stripping, and other radiometric distortion. Among many MNF components, we selected the first five MNF components of good quality. The number of MNF components are limited to 5, which is the same number of spectral bands used for the ETM+ data.

### 3.2 Selection training sites for detection of soil types

For the classification five soil types, we selected training pixels from both image data sets using the VITD maps. Total 37 training sites are selected as to minimize vegetation fraction on soil surface by visual interpretation of Hyperion color-composite images.

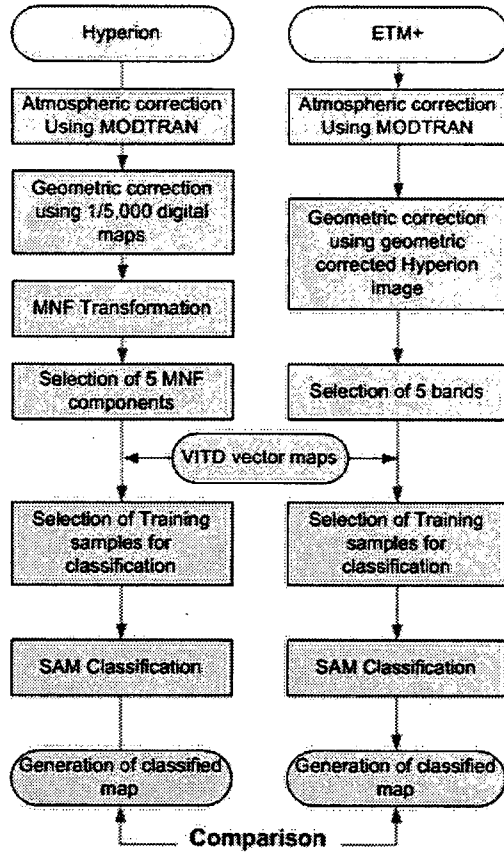


Figure 3. Processing steps of this study.

### 3.3 Classification of soil types

Classification method used for the study is the spectral angle mapper (SAM) algorithm. The SAM algorithm measured the spectral angle between the class  $t$  and the unknown pixel  $p$  and can be calculated by the following equation.

$$\alpha = \cos^{-1} \left[ \frac{\langle \vec{t}, \vec{p} \rangle}{\|\vec{t}\| \cdot \|\vec{p}\|} \right] \quad (1)$$

As the spectral angle is smaller, the unknown pixel  $t$  is defined as class  $t$ . The training sites of each soil type are defined class vectors, the every pixel of Hyperion and ETM+ image are calculated the spectral angle with these classes as equation 1. The pixel is defined as the class that the smallest angle is shown. Further, the spectral angle between input pixel and several classes is larger than the threshold value of the angle, the input pixel is classed as the undefined class.

## 4. RESULTS

Figure 4 shows the color composite of MNF components 1, 3, and 4. The MNF color composite

shows major cover types of forest, urban, and bare soil and further show the differences within bare soil area. The rice paddy area looks pink color, bright bare soil is blue color while the bare soil area and forest are distinguished by the difference in green tone. Urban area is shown as yellow color. Figure 5 shows the MNF components that have major noise fractions within the Hyperion image. The radiometric noise types observed in the Hyperion data are the smile effect the stripping.

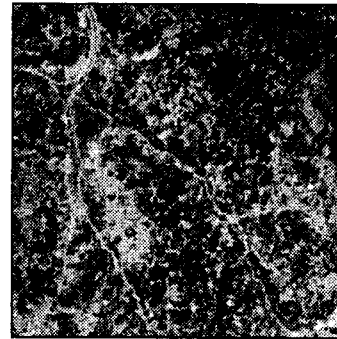


Figure 4. Color composite image of MNF 1,3,4 components of Hyperion data at subset area of site 1.

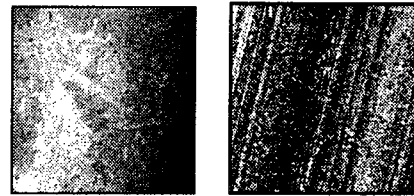


Figure 5. The noisy MNF components of Hyperion data.

Five MNF components of Hyperion image and five bands of ETM+ image are classified into four soil classes. For the study site 2, only evaporites soil was classified. Figure 6 shows the classified soil map using Hyperion (left) and ETM+ data (right) for the site 1. Table 3 shows the overall accuracy of classification and accuracy of four soil types. This accuracy is calculated by using total 43 test sites, which are independently selected from those training pixels.

Overall classification accuracy is higher when we used Hyperion data as compared to the ETM+ data. Three soil types of GM, ML, and CL are classified better using the hyperspectral data than multispectral data. Although the hyperspectral data provide better classification accuracy, it is premature to conclude yet. The two data sets of Hyperion and ETM+ are not obtained at the same time. The ETM+ data obtained in June has more spectral influence by vegetation than the Hyperion data obtained in April.

Figure 7 shows the subset of classified map of the evaporites at study site 2 by the Hyperion (left) and the ETM+ (right) image. Some area of the evaporites are misclassified into other soil types, while the urban features (such as road and buildings) are misclassified into the evaporites. As compared with the VITD data, the evaporites are well detected with the hyperspectral data.

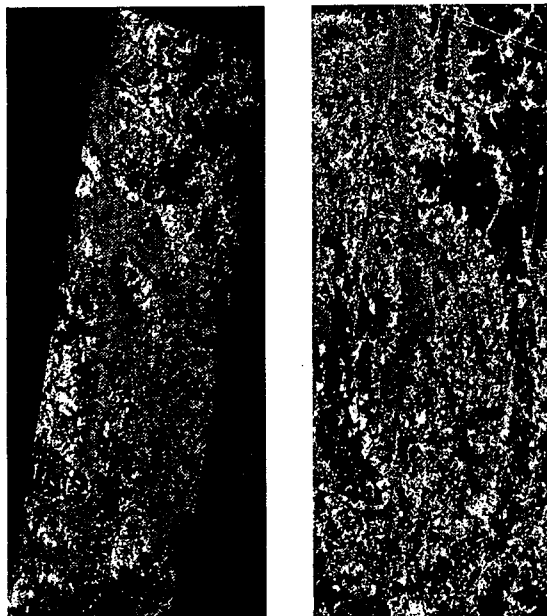


Figure 6. Soil types map of Hyperion data(left) and ETM+ data(right) by using SAM classification method.

Table 3. Classification accuracy of Hyperion and ETM+ data at site 1.

| Color | Accuracy | Hyperion | ETM+ |
|-------|----------|----------|------|
|       | Overall  |          | 81.4 |
|       | GM       | 100      | 57.1 |
|       | SM       | 50.0     | 50.0 |
|       | ML       | 78.6     | 60.0 |
|       | CL       | 92.9     | 87.5 |

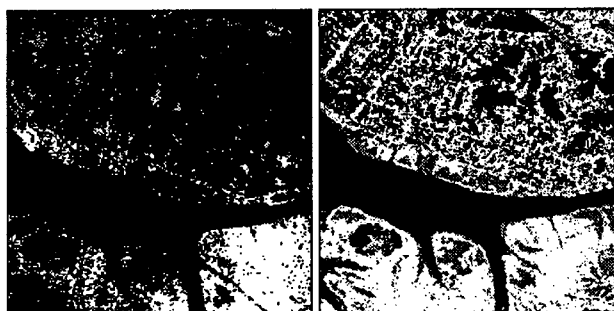


Figure 7. Subset of natural color composite image of Hyperion(upper) and evaporites maps(white-evaporites, grey-bare soil) using Hyperion (lower-left) and ETM+(lower-right) data in the study site 2.

## 5. CONCLUSIONS

In this paper, we try to test the potential of hyperspectral data for the classification of soil types defined by the VITD. From the preliminary analysis on both hyperspectral and multispectral data, the following conclusions can be made:

- The MNF transformation of the hyperspectral data is needed for removing of noise bands and reducing the number of bands for further analysis.
- Gravel, inorganic silt, clay and evaporites are classified better with the hyperspectral data than the multispectral data.
- Further study on the hyperspectral classification of soil type is planned to include more than 5 soil classes used in this study.

## References

- Ben-Dor E. et al., 2002. Mapping of several soil properties using DAIS-7915 hyperspectral scanner data-a case study over clayey soils in Israel. *INT. J. Remote Sensing*, 23(6), pp.1043-1062.
- Chabrilat S. et al., 2000. Ronda peridotite massif: methodology for its geological mapping and lithological discrimination from airborne hyperspectral data. *INT. J. Remote Sensing*. 21(12), pp.2363-2388.
- Crosta A.P. et al., 1998. Hydrothermal alteration mapping at Bodie, California, using AVIRIS hyperspectral data. *Remote Sensing of Environment*, 65, pp.309-319.
- Dehaan R. and Taylor G.R., 2003. Image-derived spectral endmembers as indicators of salinisation. *INT. J. Remote Sensing*, 24(4), pp. 775-794.
- Kruse F.A. et al., 2003. Comparison of airborne hyperspectral data and EO-1 Hyperion for mineral mapping. *IEEE Transactions on Geoscience and Remote Sensing*, 41(6), pp.1388-1400.
- Nash G.D. et al., 2004. Hyperspectral detection of geothermal system-related soil mineralogy anomalies in Dixie Valley, Nevada: a tool for exploration. *Geothermics*, 33, pp.695-711.
- Van der Meer F., 2003. Bayesian inversion of imaging spectrometer data using a fuzzy geological outcrop model. *Int. J. Remote Sensing*. 24(22), pp.4301-4310.

## Acknowledgements

This research was supported by the Agency for Defense Development, Korea, through the Image Information Research Center at Korea Advanced Institute of Science & Technology.